

Multilepton signals of gauge mediated supersymmetry breaking at the LHC

Jorgen D'Hondt^{a,b}, Karen De Causmaecker^{a,b,c}, Benjamin Fuks^{c,d},
Alberto Mariotti^e, Kentarou Mawatari^{a,b}, Christoffer Petersson^{b,f,g} and Diego Redigolo^{b,f}

^(a) *Theoretische Natuurkunde and IIHE/ELEM, Vrije Universiteit Brussel, Pleinlaan 2, B-1050 Brussels, Belgium*

^(b) *International Solvay Institutes, Brussels, Belgium*

^(c) *Theory Division, Physics Department, CERN, CH-1211 Geneva 23, Switzerland*

^(d) *Institut Pluridisciplinaire Hubert Curien/Département Recherches Subatomiques, Université de Strasbourg/CNRS-IN2P3, 23 Rue du Loess, F-67037 Strasbourg, France*

^(e) *Institute for Particle Physics Phenomenology, Durham University, Durham DH1 3LE, United Kingdom*

^(f) *Physique Théorique et Mathématique, Université Libre de Bruxelles, C.P. 231, B-1050 Brussels, Belgium*

^(g) *Department of Fundamental Physics, Chalmers University of Technology, 412 96 Göteborg, Sweden*

We investigate multilepton LHC signals arising from electroweak processes involving sleptons. We consider the framework of general gauge mediated supersymmetry breaking, focusing on models where the low mass region of the superpartner spectrum consists of the three generations of charged sleptons and the nearly massless gravitino. We demonstrate how such models can provide an explanation for the anomalous four lepton events recently observed by the CMS collaboration, while satisfying other existing experimental constraints. The best fit to the CMS data is obtained for a selectron/smuon mass of around 145 GeV and a stau mass of around 90 GeV. These models also give rise to final states with more than four leptons, offering alternative channels in which they can be probed and we estimate the corresponding production rates at the LHC.

I. INTRODUCTION

Despite the tremendous success of the Standard Model (SM) of particle physics, the SM leaves many questions unanswered and it hints toward the existence of new physics around the TeV scale. The arguably strongest hint, which is reinforced by the recent observation of a Higgs boson at the Large Hadron Collider (LHC) [1, 2], arises from the quadratic sensitivity of the Higgs mass parameter to physics beyond the SM. This so-called hierarchy problem is addressed by weak scale supersymmetry [3, 4]. Relating fermionic and bosonic degrees of freedom, supersymmetry (SUSY) not only stabilizes the weak scale but can also provide an explanation for dark matter in the Universe and give rise to gauge coupling unification at high energies. Consequently, searches for the superpartners of the SM particles play key roles in the experimental program at the LHC.

The ATLAS and CMS collaborations have so far focused mainly on analyzing signatures arising from the strong production of squarks and gluinos. However, the negative search results have increased the interest in analyses of the production of the electroweak superpartners, whose cross sections are much smaller than colored ones. Consequently, both collaborations have recently, for the first time, been able to put bounds on these particles that are stronger than those extracted from LEP data, as shown, *e.g.*, in Refs. [5, 6].

In this letter we consider the framework of gauge-mediated SUSY breaking (see Ref. [7] for a review and original references) in its general formulation (GGM) [8], where it is possible to construct models in which all the colored superpartners are heavy but some (or all) of the

electroweak superpartners are light. One benefit of this kind of spectrum is that a 125 GeV Higgs boson can be easily accommodated by means of multi-TeV top squarks.

We focus on models in which the three generations of right-handed sleptons, together with the nearly massless gravitino, are in the low mass region of the superpartner spectrum. Such models can be probed at the LHC by analyzing events originating from the pair-production of sleptons that decay promptly into lepton-rich final states with missing transverse energy \cancel{E}_T carried by gravitinos.

We show that some of these GGM models can provide an explanation for a possible anomalous production of events with four leptons recently observed by the CMS collaboration [9]. We also discuss the compatibility with the constraints extracted from the dilepton+ \cancel{E}_T searches at both LEP and LHC experiments, as well as from other LHC multilepton searches. We finally propose, for the model that fits the data best, additional signatures that could be searched for using both data from the previous LHC runs and future data from the run at a center-of-mass energy of $\sqrt{s} = 13$ TeV.

II. THEORETICAL FRAMEWORK AND BENCHMARK SCENARIOS

We consider a class of GGM models where the selectron and smuon (generically referred to as sleptons in the following), as well as the stau, lie in the low-mass range of the superparticle spectrum. Moreover, as for any scenario where SUSY breaking is mediated by gauge interactions [7], the lightest supersymmetric particle (LSP) is the gravitino, whose typical mass is $\mathcal{O}(\text{eV})$ for SUSY-

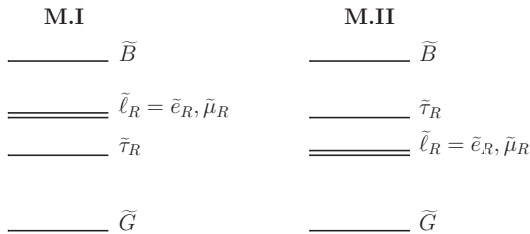


FIG. 1: Mass spectra for our simplified model of type **M.I** (left) and **M.II** (right). In **M.I** scenarios, the stau $\tilde{\tau}_R$ is the NLSP and the right-handed selectron/smuon $\tilde{\ell}_R$ are co-NNLSP. In models of class **M.II**, the situation is reversed.

breaking scales of $\mathcal{O}(100 \text{ TeV})$.

Adopting a bottom-up approach for new physics, we investigate the phenomenology of a simplified model in which we extend the SM field content by adding a nearly massless gravitino \tilde{G} , a pair of mass-degenerate right-handed sleptons $\tilde{\ell}_R = \tilde{e}_R, \tilde{\mu}_R$ and a (for simplicity, non-mixed) stau $\tilde{\tau}_R$. In addition, we also include the lightest neutralino state, considered to be bino-like and heavier than both the sleptons and the stau. All the remaining superpartners are assumed to be heavy and effectively decoupled. Similar scenarios were considered in Refs. [10, 11].

In this simplified model, two possible hierarchies can be realized in the slepton/stau sector. As presented in Fig. 1, we consider both of these and denote by **M.I** scenarios where the stau is the next-to-lightest superparticle (NLSP) and sleptons the next-to-next-to-lightest superpartners (NNLSP), and by **M.II** scenarios with an inverted hierarchy, with the sleptons being co-NLSP and the stau the NNLSP. While models of type **M.I** are typical in GGM (even in minimal gauge mediation), models of type **M.II** can be realized when the soft masses for both Higgs fields at the UV scale are allowed to receive extra, non-gauge mediated, contributions [12, 13].

Slepton pairs are produced via the electroweak Drell-Yan process. Due to the steeply falling cross section with increasing slepton masses [14], we consider slepton and stau masses only up to 300 GeV, a range above which it is unlikely that the LHC at $\sqrt{s} = 8 \text{ TeV}$ is sensitive. This is illustrated in Fig. 2 where we present the production cross section of a right-handed slepton/stau pair at the LHC, for $\sqrt{s} = 8 \text{ TeV}$ and 13 TeV , as computed by RESUMMINO [15–18].

For both types of scenarios, the NLSP universally decays directly into a gravitino and the corresponding SM partner,

$$\tilde{\tau}_R \rightarrow \tau \tilde{G} \text{ (M.I); } \quad \tilde{\ell}_R \rightarrow \ell \tilde{G} \text{ (M.II)}, \quad (1)$$

with a decay length depending on the gravitino mass [7]. We require this decay to be prompt so that an upper bound on the gravitino mass is imposed at around 10 eV.

Concerning the NNLSP, the analogous two-body decay competes with possible three-body decay modes via an

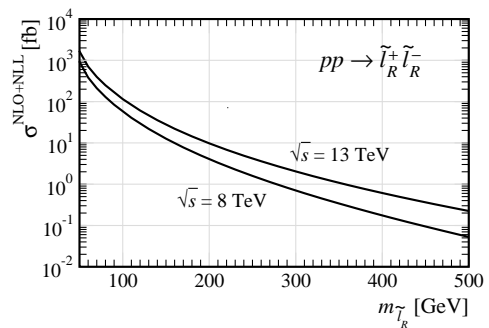


FIG. 2: Right-handed slepton/stau pair-production cross section at the LHC, for a single flavor, as a function of the slepton mass.

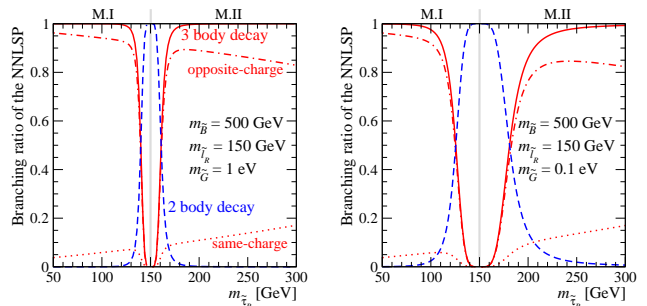


FIG. 3: Branching ratio of the NNLSP as a function of the stau mass for two different choices of the gravitino mass, $m_{\tilde{G}} = 1 \text{ eV}$ (left) and 0.1 eV (right), where the bino and slepton masses are fixed at 500 GeV and 150 GeV, respectively. The dashed red line corresponds to the two-body decay to the gravitino, while the solid blue line indicates the total three-body decay branching ratio. The red dashed-dotted and dotted lines represent the opposite-charge and same-charge three-body decays, respectively, as explained in the text.

off-shell bino,

$$\tilde{\ell}_R \rightarrow \ell \tau \tilde{\tau}_R \text{ (M.I); } \quad \tilde{\tau}_R \rightarrow \tau \ell \tilde{\ell}_R \text{ (M.II)}. \quad (2)$$

Fig. 3 presents, for two different choices of the gravitino mass $m_{\tilde{G}} = 1 \text{ eV}$ (left) and 0.1 eV (right), the NNLSP two-body and three-body branching ratios when fixing the bino mass to 500 GeV, the slepton mass $m_{\tilde{\ell}_R}$ to 150 GeV and when varying the stau mass $m_{\tilde{\tau}_R}$. When $m_{\tilde{\tau}_R} < m_{\tilde{\ell}_R}$ (**M.I**), we display the decay modes of the slepton, whereas when $m_{\tilde{\tau}_R} > m_{\tilde{\ell}_R}$ (**M.II**) the ones of the stau. The three-body decay is found dominant except in the region where the NNLSP and NLSP are close in mass ($m_{\tilde{\tau}_R} \approx m_{\tilde{\ell}_R}$). This result is robust under variations of the bino mass.

We briefly notice that the three-body decay distinguishes between the different charge channels, *i.e.*, the NLSP can have either the opposite charge of the NNLSP ($\tilde{\ell}_R^- \rightarrow \ell^- \tau^- \tilde{\tau}_R^+$) or the same ($\tilde{\ell}_R^- \rightarrow \ell^- \tau^+ \tilde{\tau}_R^-$) [10], denoted by dashed-dotted and dotted lines in Fig. 3. Generically, the more the bino is off-shell, the more the opposite charge channel dominates. Since the dominance of one

channel with respect to the other is very much dependent on whether the sleptons are right- or left-handed, on the amount of stau mixing and on the nature of the neutralino, a detailed analysis of these effects might give us a way of probing non-trivial properties of the spectrum. However, the current LHC statistics is too low to allow for this analysis that we leave for further investigation.

III. MULTILEPTON SIGNALS IN GAUGE MEDIATED SUPERSYMMETRY BREAKING

Recently the CMS collaboration reported a slight excess in events with three electrons or muons (out of which one opposite-sign same flavor lepton pair can be formed) and one hadronically decaying tau, in the category with a Z -veto, low hadronic activity and no jet issued from the fragmentation of a b -quark [9]. With 19.5 fb^{-1} of collisions at $\sqrt{s} = 8 \text{ TeV}$, the number of observed (expected) events in this category is 15 (7.5 ± 2), 4 (2.1 ± 0.5) and 3 (0.6 ± 0.24) for the three regions $\cancel{E}_T < 50 \text{ GeV}$, $\cancel{E}_T \in [50, 100] \text{ GeV}$ and $\cancel{E}_T > 100 \text{ GeV}$, respectively.

Motivated by this result, we investigate the contributions arising from slepton and stau pair production for models of class **M.I** and **M.II**. To display our results, we fix the bino and gravitino masses to 500 GeV and 1 eV, respectively, and scan the slepton and stau masses from 50 GeV to 300 GeV. Within our choice of parameters, the NNLSP dominantly decays via its three-body mode in most of the $(m_{\tilde{\ell}_R}, m_{\tilde{\tau}_R})$ mass plane. This allows for a possible enhancement of the production rates of final states comprised of $4\tau + 2\ell + \cancel{E}_T$ and $2\tau + 4\ell + \cancel{E}_T$ for **M.I** and **M.II** scenarios, respectively, as depicted in Fig. 4. The actual final state lepton multiplicity however depends on the number of leptonically decaying taus.

For our SUSY signal simulation, we use the goldstino model [19, 20] implemented in the FEYNRULES package [21, 22] and export it to a UFO library [23] which has been linked to MADGRAPH 5 [24]. The generated parton-level events have then been processed by PYTHIA [25] for parton showering and hadronization, TAUOLA [26] for tau decays and by DELPHES [27] for detector simulation using the recent CMS detector description of Ref. [28]. We have analyzed 19.5 fb^{-1} of events describing NNLSP pair production at the LHC, running at $\sqrt{s} = 8 \text{ TeV}$, with MADANALYSIS 5 [29]. Generated events have been reweighted using signal cross sections predicted by RESUMMINO at the next-to-leading order and next-to-leading logarithmic accuracy, as shown in Fig. 2. This results in typical K -factors of about 1.2 for the scanned mass range.

For event selection, we follow the CMS multilepton analysis of Ref. [9] and base our results on an investigation of the properties of isolated electron and muon candidates whose transverse-momentum p_T is greater than 10 GeV and pseudorapidity $|\eta|$ is smaller than 2.4. We enforce lepton isolation by imposing the amount of transverse activity in a cone of radius $R = \sqrt{\Delta\varphi^2 + \Delta\eta^2} = 0.3$ centered on the lepton, φ being the azimuthal angle with

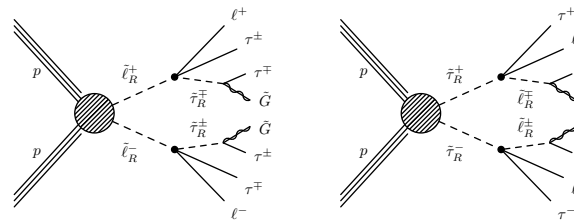


FIG. 4: Diagrams leading to multilepton production in association with missing energy in scenarios of type **M.I** (left) and **M.II** (right).

respect to the beam direction, to be less than 15% of the lepton p_T . Additionally, we impose the leading lepton (electron or muon) transverse momentum to satisfy $p_T > 20 \text{ GeV}$ and include efficiencies of 95%, 93% and 90% to simulate the effects of the double-electron, electron-muon and double-muon triggers relevant for the considered final state topologies. Finally, events featuring a pair of opposite-sign same flavor (OSSF) leptons whose invariant-mass is smaller than 12 GeV are rejected. While leptonically-decaying taus are accounted for as the electrons or muons in which they decay into, hadronically-decaying taus τ_h are reconstructed as such and we demand their visible p_T to be greater than 20 GeV and their pseudorapidity to fulfill $|\eta| < 2.3$.

The CMS analysis classifies events as having H_T greater or less than 200 GeV as well as counting the number of b -tagged jets in the final states for which we employ the b -tagging algorithm described in Ref. [28]. The H_T variable is defined as the scalar sum of the transverse energy of all isolated reconstructed jets with $p_T > 30 \text{ GeV}$ and $|\eta| < 2.5$, for which we use an anti- k_T algorithm whose radius parameter is fixed to $R = 0.5$ [30], as implemented in the FASTJET package [31], and we consider a jet as isolated only if no electron, muon or tau lies within a cone of radius $R = 0.3$ centered on the jet. Concerning signal events, the hadronic activity mainly arises from initial state radiation so that H_T is always found smaller than 200 GeV and the number of b -jets is rarely above zero. This feature is actually welcome since the CMS experiment does not see any excess in the regions where $H_T > 200 \text{ GeV}$ or $N_{b\text{-jets}} \geq 1$.

After applying the above requirements, events with at least three leptons are selected, where at most one of them is a hadronic tau. Further categories are made by classifying each event in terms of the maximum number of opposite-sign same flavor (OSSF) lepton pairs. Final state signatures predicted by both **M.I** and **M.II** models contain at least one OSSF lepton pair in most of the parameter space, which is again a welcome feature since the bins with zero OSSF lepton pairs do not exhibit any excess. The ‘on- Z ’ region is populated if at least one OSSF lepton pair has an invariant mass in the Z -window $|m_{\ell+\ell} - m_Z| < 15 \text{ GeV}$ while in the ‘off- Z ’ region, each OSSF dilepton invariant mass has to lie outside the Z -window.

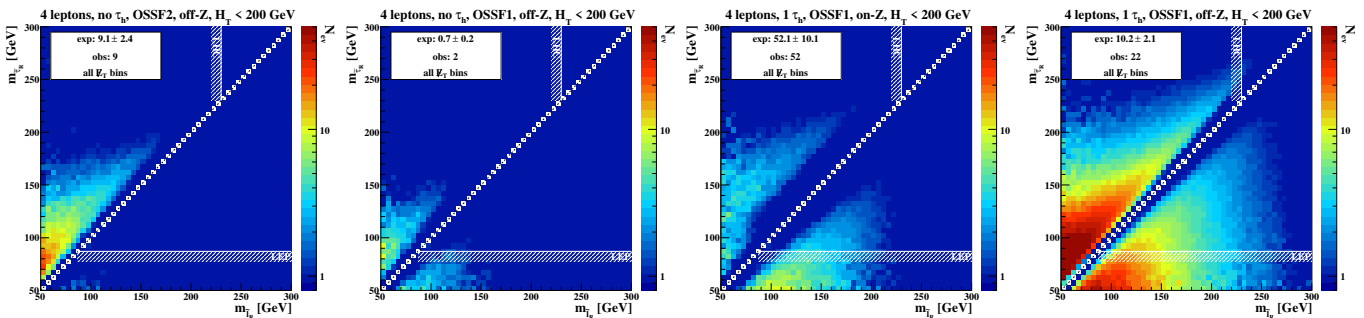


FIG. 5: Number of the signal event in the $(m_{\tilde{\ell}_R}, m_{\tilde{\tau}_R})$ plane for some representative categories, after summing \cancel{E}_T bins. The numbers of expected and observed events are also presented [9], as well as LEP and LHC bounds from direct slepton searches.

After summing the \cancel{E}_T bins, we have six categories for both the four lepton and the three lepton cases. We focus our discussion mainly on the four lepton channels since in the three leptons ones, the expected background is so large that the contributions from our signal region, characterized by a small yield, are always in agreement with the expectation within the statistical precision.

For illustrative purposes, in Fig. 5 we show four categories out of the possible six for the four lepton case, displaying the number of signal events in the $(m_{\tilde{\ell}_R}, m_{\tilde{\tau}_R})$ mass plane. We also quote the numbers of expected and observed events from Table 2 in the CMS note [9]. The lower half plane, with $m_{\tilde{\tau}_R} < m_{\tilde{\ell}_R}$, corresponds to the **M.I** models, while the upper half plane, with $m_{\tilde{\tau}_R} > m_{\tilde{\ell}_R}$, corresponds to the **M.II** models.

In the category with two ‘off- Z ’ OSSF lepton pairs, corresponding to the first panel of Fig. 5, the CMS analysis finds good agreement with the SM expectation. While models of class **M.I** do not give rise to any signal events in this category, the **M.II** models that are best compatible with the data in this category are those with $m_{\tilde{\tau}_R} \gtrsim 150$ GeV, *i.e.* those that give rise to very few signal events. The category with one ‘off- Z ’ pair of OSSF leptons and no hadronic tau is shown as the second panel of Fig. 5. For very low stau masses, **M.I** scenarios can populate this bin with events featuring at least two leptonically decaying taus. By comparing with the first panel of the figure, we observe that out of the four leptons, **M.I** models generally predict, in the absence of hadronic taus, that one single OSSF lepton pair can be formed, whereas two OSSF lepton pairs are rather expected in **M.II** models. In the third panel of Fig. 5, we turn to the four lepton category including one hadronic tau and where one single OSSF lepton pair can be formed and lies in the Z -window. All scanned **M.I** and **M.II** scenarios predict number of events lying comfortably within 1σ variation of the SM expectation. The last panel of Fig. 5 shows the four lepton category including one hadronic tau and one OSSF lepton pair whose invariant mass is not compatible with the Z -boson mass. This category corresponds to the observed excess and both types of signal scenarios can provide good candidates for explaining it.

In Fig. 6, we display the precise distribution of our signal in the different \cancel{E}_T bins corresponding to the last panel of Fig. 5. Scenarios of class **M.I** do not populate the bin with $\cancel{E}_T > 100$ GeV, unless in a narrow region where the stau is very light. Performing a χ^2 fit restricted to the three bins displayed in the figure for both class of models, the best benchmark scenarios are given by

$$\mathbf{M.I} : m_{\tilde{\ell}_R} = 140 \text{ GeV}, m_{\tilde{\tau}_R} = 50 \text{ GeV}, \chi_{\text{exc.}}^2 = 1.22 ;$$

$$\mathbf{M.II} : m_{\tilde{\ell}_R} = 50 \text{ GeV}, m_{\tilde{\tau}_R} = 140 \text{ GeV}, \chi_{\text{exc.}}^2 = 2.28 .$$

Both models end up providing an explanation for the excess. However, as detailed below, experimental constraints arising from direct NLSP pair production exclude all **M.II** candidates explaining the excess, and have also non-trivial consequences on the best fit for **M.I** models.

In **M.II** models, where the right-handed sleptons are co-NLSP, current bounds on the slepton mass apply, $m_{\tilde{\ell}_R} > 230$ GeV [5, 6]. These bounds are extracted from slepton pair production and subsequent decay into a lepton and a gravitino (a nearly massless LSP). As indicated in both Figs. 5 and 6, this excludes the entire region of the **M.II** parameter space possibly relevant for explaining the CMS excess. On the other hand, for **M.I** scenarios in which the right-handed stau is the NLSP, the most stringent constraints are those set by LEP experiments, $m_{\tilde{\tau}_R} > 87$ GeV [32], as the corresponding LHC searches have a too low sensitivity [33]. Consequently, **M.I** models still provide viable candidates for explaining the excess.

The point of the **M.I** parameter space ending up to be the best fit of the three bins with the excess becomes, after accounting for LEP limits on the stau mass,

$$m_{\tilde{\ell}_R} = 145 \text{ GeV}, m_{\tilde{\tau}_R} = 90 \text{ GeV}, \chi_{\text{exc.}}^2 = 2.42 ,$$

where $m_{\tilde{\tau}_R}$ lies at the edge of the excluded region. The significance of our best fit scenario is found reduced as signal contributions to the low missing energy bin of Fig. 6 are smaller for larger stau masses. This further motivates us to study in detail how and whether LHC direct searches could improve LEP limits on the stau mass [34]. As a crosscheck of our reasoning, we perform a global fit on the **M.I** parameter space including all four leptons

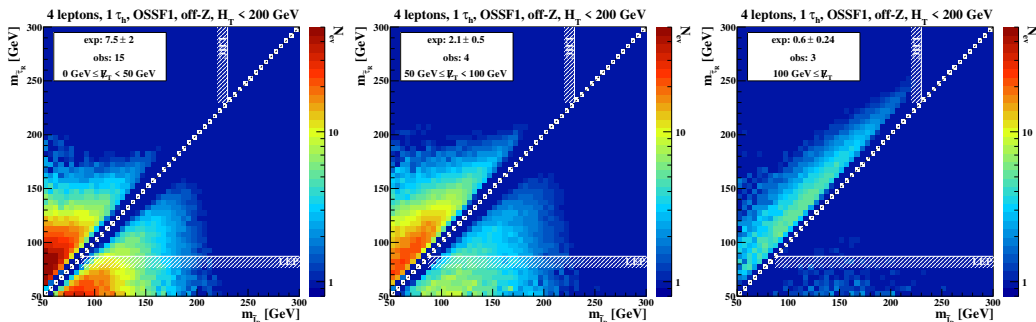


FIG. 6: The same as in Fig. 5, but for a category where the excess events are observed and for different \cancel{E}_T bins.

categories. Not surprisingly, the same best fit benchmark point with $m_{\tilde{\tau}_R} = 90$ GeV and $m_{\tilde{\ell}_R} = 145$ GeV is obtained.

Focusing from now on on the best fit point, we briefly comment on other signatures that it induces and which could be probed through other multilepton searches at the LHC. Firstly, CMS searches for R -parity violating (RPV) SUSY in leptonic final states are not expected to be sensitive to such models as it requires four electron or muons in the final states [35]. Such a signature is suppressed in the framework of **M.I** models (as already shown on the first panel of Fig. 5) as it requires at least two of the taus to decay leptonically.

Secondly, the ATLAS collaboration has recently performed a multilepton search which features one signal region, dubbed ‘SR1noZ’, that might be relevant for models of class **M.I** [36]. This analysis has been designed for RPV SUSY searches and requires exactly three electrons or muons and at least one tau. An extended Z -veto is demanded so that events with a lepton pair, triplet or quadruplet whose invariant mass lies within a 20 GeV interval centered on the Z -boson mass are rejected. The search strategy additionally requires either a selection on the missing energy $\cancel{E}_T > 100$ GeV or on the effective mass, defined as the sum of the missing energy and of all the transverse momenta of the reconstructed final state objects (leptons, hadronic taus, jets), $m_{\text{eff}} > 400$ GeV. On the one hand, our signal does not populate the $\cancel{E}_T > 100$ GeV category as shown on Fig. 6. On the other hand, the tail of the effective mass distribution for our best benchmark point has been found to only extend up to about 350 GeV, which can be heuristically understood as most of the reconstructed final state objects come from the decay of a slepton pair with an invariant mass of about 300 GeV. This ATLAS search is therefore expected to be insensitive to our benchmark.

Lastly, the ATLAS collaboration has recently performed an investigation of ditau events [33], making use of a dedicated trigger on two reconstructed hadronic taus. This analysis could be relevant in our case since the signal is likely to populate bins with two hadronic taus, as shown in Table I. However, these taus are always accompanied by extra electrons or muons issued from NNLSP three-body decays, so that no hint in the ATLAS signal

$N(\ell)$	$N(\tau_h)$	$N_{\text{events}}(8 \text{ TeV})$	$N_{\text{events}}(13 \text{ TeV})$
4	2	22.5	223
5	0	0.074	0.79
5	1	1.7	14.7
5	2	7.4	76.1
6	0	0	0
6	1	0.075	0.66
6	2	1.0	7.89
> 6	0	0.038	13.9

TABLE I: Number of multilepton events N_{events} predicted by the scenario that fits the CMS excess best (**M.I** model, $m_{\tilde{\ell}} = 145$ GeV, $m_{\tilde{\tau}} = 90$ GeV). The third column corresponds to 19.5 fb^{-1} of LHC collisions at $\sqrt{s} = 8$ TeV and the fourth column to 100 fb^{-1} of LHC collisions at $\sqrt{s} = 13$ TeV. Moreover, $N(\ell)$ denotes the total number of charged leptons and $N(\tau_h)$ how many of these are hadronically-decaying taus.

regions, which also include a veto on additional leptons, is foreseen.

Let us finally discuss how some of the existing searches can be optimized to improve their sensitivity for signal scenarios of class **M.I**. As an illustrative example, we show in Table I that our best fit point is considerably contributing to final states with two hadronically decaying taus plus either two or three electrons or muons. In particular, predicting a considerably large number of events featuring three electrons or muons shows that the lepton abundance in the final state can be considerably enhanced by the leptonically decaying taus, even though the associated branching fraction is reduced. For these reasons we point out that an optimized search strategy for **M.I** models should impose selections on the lepton multiplicity as inclusive as possible, as already suggested in the context of optimizing Tevatron searches for gauge mediation scenarios [11]. Moreover, one peculiar feature of our benchmark scenario is the presence of at least two hadronically decaying taus which are hard enough to be reconstructed. We therefore suggest an effective search dedicated to **M.I** scenarios that could be made by combining triggers on two hadronically decaying taus with a binning on the number of extra leptons in the final state.

IV. CONCLUSIONS

In this letter, we have investigated the phenomenology of models involving light charged sleptons, realized within the framework of general gauge mediated supersymmetry breaking. Motivated by the recent CMS observation of an excess in multilepton events, we have demonstrated that some of these models can not only provide an explanation for the excess but also explain why no hint of new physics has been found in other leptonic searches by both the ATLAS and CMS collaborations. We have shown that the model that best fits the data, and which is compatible with all current experimental constraints, involves right-handed selectrons and smuons of 145 GeV and a right-handed stau of 90 GeV. The presence of a light stau at the edge of the LEP limit in our benchmark motivates further investigation about the possible impact of LHC searches on the stau mass bound [34]. Finally, we proposed new investigations in multileptonic channels that could probe this type of GGM models and further constrain them in the future.

Acknowledgments

The work of B.F. has been partially supported by the Theory-LHC France-initiative of the CNRS/IN2P3 and by the French ANR 12 JS05 002 01 BATS@LHC. J.D.H., K.D.C. and K.M. are supported in part by the Belgian Federal Science Policy Office through the Interuniversity Attraction Pole P7/37 and in part by the Strategic Research Program “High Energy Physics” and the Research Council of the Vrije Universiteit Brussel. K.D.C. is also partially supported by a “FWO-Vlaanderen” aspirant fellowship and acknowledges the hospitality of the CERN TH group and the support from the ERC grant 291377 “LHCtheory: Theoretical predictions and analyses of LHC physics: advancing the precision frontier”. The work of C.P. and D.R. was supported in part by IISN-Belgium (conventions 4.4511.06, 4.4505.86 and 4.4514.08), by the “Communauté Française de Belgique” through the ARC program and by a “Mandat d’Impulsion Scientifique” of the F.R.S.-FNRS. A.M. acknowledges funding by the Durham International Junior Research Fellowship.

-
- [1] G. Aad et al. (ATLAS Collaboration), *Phys.Lett* **B716**, 1 (2012).
 - [2] S. Chatrchyan et al. (CMS Collaboration), *Phys.Lett* **B716**, 30 (2012).
 - [3] H. P. Nilles, *Phys.Rept.* **110**, 1 (1984).
 - [4] H. E. Haber and G. L. Kane, *Phys.Rept.* **117**, 75 (1985).
 - [5] ATLAS Collaboration (2013), ATLAS-CONF-2013-049.
 - [6] CMS Collaboration (2013), CMS-PAS-SUS-13-006.
 - [7] G. Giudice and R. Rattazzi, *Phys.Rept.* **322**, 419 (1999).
 - [8] P. Meade, N. Seiberg, and D. Shih, *Prog.Theor.Phys.Suppl.* **177**, 143 (2009).
 - [9] CMS Collaboration (2013), CMS-PAS-SUS-13-002.
 - [10] S. Ambrosanio, G. D. Kribs, and S. P. Martin, *Nucl.Phys.* **B516**, 55 (1998).
 - [11] J. T. Ruderman and D. Shih, *JHEP* **1011**, 046 (2010).
 - [12] J. L. Evans, D. E. Morrissey, and J. D. Wells, *Phys.Rev.* **D75**, 055017 (2007).
 - [13] P. Grajek, A. Mariotti, and D. Redigolo, *JHEP* **1307**, 109 (2013).
 - [14] W. Beenakker, M. Klasen, M. Kramer, T. Plehn, M. Spira, et al., *Phys.Rev.Lett.* **83**, 3780 (1999).
 - [15] G. Bozzi, B. Fuks, and M. Klasen, *Phys.Rev.* **D74**, 015001 (2006).
 - [16] G. Bozzi, B. Fuks, and M. Klasen, *Nucl.Phys.* **B777**, 157 (2007).
 - [17] G. Bozzi, B. Fuks, and M. Klasen, *Nucl.Phys.* **B794**, 46 (2008).
 - [18] B. Fuks, M. Klasen, D. R. Lamprea, and M. Rothering, *Eur.Phys.J.* **C73**, 2480 (2013).
 - [19] R. Argurio, K. De Causmaecker, G. Ferretti, A. Mariotti, K. Mawatari, et al., *JHEP* **1206**, 096 (2012).
 - [20] K. Mawatari and Y. Takaesu, *Eur.Phys.J.* **C71**, 1640 (2011).
 - [21] N. D. Christensen and C. Duhr, *Comput.Phys.Commun.* **180**, 1614 (2009).
 - [22] C. Duhr and B. Fuks, *Comput.Phys.Commun.* **182**, 2404 (2011).
 - [23] C. Degrande, C. Duhr, B. Fuks, D. Grellscheid, O. Mattelaer, et al., *Comput.Phys.Commun.* **183**, 1201 (2012).
 - [24] J. Alwall, M. Herquet, F. Maltoni, O. Mattelaer, and T. Stelzer, *JHEP* **1106**, 128 (2011).
 - [25] T. Sjostrand, S. Mrenna, and P. Z. Skands, *JHEP* **0605**, 026 (2006).
 - [26] S. Jadach, Z. Was, R. Decker, and J. H. Kuhn, *Comput.Phys.Commun.* **76**, 361 (1993).
 - [27] S. Oryn, X. Rouby, and V. Lemaitre (2009), 0903.2225.
 - [28] J.-L. Agram, J. Andrea, E. Conte, B. Fuks, D. Gelé, et al., *Phys. Lett.* **B725**, 123 (2013).
 - [29] E. Conte, B. Fuks, and G. Serret, *Comput.Phys.Commun.* **184**, 222 (2013).
 - [30] M. Cacciari, G. P. Salam, and G. Soyez, *JHEP* **0804**, 063 (2008).
 - [31] M. Cacciari, G. P. Salam, and G. Soyez, *Eur.Phys.J.* **C72**, 1896 (2012).
 - [32] G. Abbiendi et al. (OPAL Collaboration), *Eur.Phys.J.* **C46**, 307 (2006).
 - [33] ATLAS Collaboration (2013), ATLAS-CONF-2013-028.
 - [34] J. D’Hondt, K. De Causmaecker, B. Fuks, A. Mariotti, K. Mawatari, C. Petersson, and D. Redigolo (to appear).
 - [35] CMS Collaboration (2013), CMS-PAS-SUS-13-010.
 - [36] ATLAS Collaboration (2013), ATLAS-CONF-2013-036.